

Electronic Structure of an Organic/Metal Interface: Pentacene/Cu(110)

Kathrin Müller,^{†,⊥} Ari P. Seitsonen,[‡] Thomas Brugger,[§] James Westover,^{||} Thomas Greber,[§] Thomas Jung,[†] and Abdelkader Kara^{*,||}

[†]Laboratory for Micro- and Nanotechnology, Paul Scherrer Institut, CH-5232 Villigen PSI, Switzerland

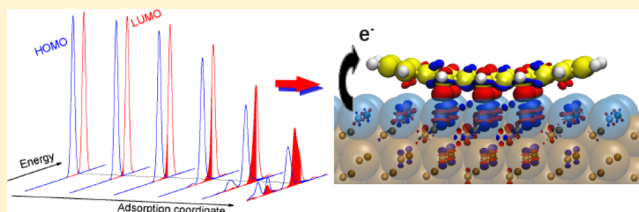
[‡]Physikalisch-Chemisches Institut, University of Zurich, Winterthurerstrasse 190, CH-8057 Zurich, Switzerland

[§]Physik-Institut, University of Zurich, CH-8057 Zürich, Switzerland

^{||}Department of Physics, University of Central Florida, Orlando, Florida 32816, United States

Supporting Information

ABSTRACT: A detailed understanding of the organic molecule/substrate interface is of crucial importance for the design of organic semiconducting devices, as the interface determines the contact resistance and the charge injection. Generally, two different adsorption situations are considered: physisorption and chemisorption. For small molecular adsorbates like CO or N₂, the adsorption energy alone can be used as a criterion to classify the adsorption in chemisorption (adsorption energies larger than 1 eV) and physisorption (few tens of meV). This classification fails for complex π -conjugated organic molecules. Here we discuss on the basis of a pentacene/Cu(110) model system a different set of criteria to distinguish between chemisorption and physisorption beyond the total bond energy argument. We analyze the bonding situation on the basis of density functional theory (DFT) calculations and photoelectron spectroscopy. Theory predicts (i) a significant bending of the molecule after adsorption, (ii) a buckling of the top layer Cu atoms, (iii) the emergence of new hybrid states, and (iv) a substantial charge redistribution and accompanying charge transfer. Photoemission confirms the energies of the 3 topmost molecular orbitals with an almost “half-filled” lowest unoccupied molecular orbital (LUMO). The four criteria are used to qualify the adsorption mechanism in the pentacene/Cu(110) system as chemisorption. This set of criteria is indicative of chemisorption also in the case of other noncovalently coupled large adsorbates, far beyond the pentacene/Cu(110) case.



INTRODUCTION

The last two decades have witnessed an increasing interest in organic materials for the fabrication of low-cost, flexible, lightweight, and durable electronic devices. Such devices^{1,2} include organic light emitting diodes (OLED), organic field-effect transistors (OFET), organic thin-film transistors (OTFT), and organic photovoltaic (OPV) solar cells. Emerging only recently, there is also a high interest to use organic materials and their interfaces for spintronics.^{3–5} A detailed scrutiny of the interface between the organic semiconductors and their contacting substrates is of great importance,^{6–9} as this interface affects the density of states,¹⁰ the contact resistance,¹¹ and the charge or spin injection property of the device. The organic molecules and the metallic substrate exhibit electronic structures of very distinct nature. This constitutes a complex system with characteristic properties which may depend on the kind of bonding at the interface, i.e., on whether it is predominantly of physisorption or chemisorption type, next to other material parameters. The nature of the bonding via the electronic interaction between the atomic and/or molecular orbitals and substrate states is crucial in determining the electronic contact between molecules and a metal substrate,

and provides a key to designing the electronic and magnetic¹² properties of these interfaces. It was also shown recently that detailed knowledge of the adsorbate/substrate interaction as well as of the interface morphology is a prerequisite to choose the correct model toward a theoretical description of the interface.⁹

Many small adsorbates predominantly bind to the substrate in an atomically confined way, which allows for the assumption of a single weak or strong bond. In this simple case, the overall interaction energy is predictive on whether the bond across the interface is weak, dominated by van der Waals interaction and can thus be qualified as physisorption, or strong, dominated by a directional chemical bond, i.e., by chemisorption. In this case, information about the binding energy is enough to categorize the bonding—a few tens of meV's vs a few eV's would classify the first case as physisorption and the second case as chemisorption.¹³ In some cases like N₂/W(110),¹⁴ the molecule physisorbs on the surface (keeping its structural

Received: August 13, 2012

Revised: October 10, 2012

Published: October 15, 2012

integrity) or dissociates where the fragments chemisorb on the surface (hence, the molecule loses its structural integrity). In the different case of organic molecules containing large delocalized orbitals, the bonding situation is recognized to be more complex.¹⁵ For pentacene on Cu(110), it was stated¹⁶ that the adsorption is neither compatible with the case of pure physisorption nor with pure chemisorption. This is an example of a case where the conventional classification scheme between physisorption and chemisorption seems to fail: If it is applied to organic molecules with large π -systems ranging from pentacene via larger porphyrins and phthalocyanines to electronically conductive polymers. However, we consider “physisorbed” and “chemisorbed” molecules not to be disjunct sets, since every adsorbed molecule undergoes van der Waals interaction and static polarization, i.e., physisorption-type interactions, with any substrate.

For molecules containing delocalized electronic systems, the large polarizability implies a considerable interaction irrespective of whether a direct covalent bond is formed or whether an electron is transferred, where these two are considered examples for chemisorption. Another important aspect is whether electronic states are broadened or split, or whether hybrid electronic states are formed upon interaction of the adsorbate with the substrate at the interface, which indicate a stronger interaction and improve the electronic contact.

In this work, density functional theory (DFT) calculations reveal (1) the atomic arrangement of the interface between a pentacene monolayer and Cu(110), (2) the adsorbate/substrate bonding, and (3) the localization of the electronic states at the interface, which is (4) reflected in the energies of the hybrid orbitals between the molecule and the substrate. Photoelectron spectroscopy confirms these findings. For chemisorption, at least one of the atoms of the adsorbate undergoes a local chemical interaction with a substrate atom, a process which affects the valence electrons of the adsorbate as well as of the substrate. Therefore, the electronic integrity of the molecule is modified as compared to the gas phase and new interface states may emerge. Generally, such interactions may lead to a change of the molecular conformation¹⁷ and to rearrangements of the surface atoms. Adsorbate induced reconstructions¹⁸ have also been reported for large molecules, in particular on open surfaces like the [110] facet.^{17,19,20} The modified electronic states on both sides of the interface are accompanied by charge redistribution and/or charge transfer, which affect the interface dipole and modify the work function. Here, we use pentacene on Cu(110) as a model system to discuss the chemical and physical interactions for the particular case of a large technologically interesting molecule forming an organic semiconductor/metal interface and discuss a set of criteria toward the assessment and categorization of the bonding situation at such interfaces in general.

■ EXPERIMENTAL AND THEORETICAL METHODS

The experiments have been performed in a modified VG Escalab220 system²¹ with a base pressure below 1×10^{-9} mbar. The Cu(110) single-crystal has been cleaned by repeated sputter/anneal cycles until carbon and oxygen peaks were below the noise level in X-ray photoelectron spectroscopy (XPS) experiments. Pentacene molecules have been sublimed from a home-built Knudsen cell, while the sample has been kept at room temperature. XPS and low-energy electron diffraction (LEED) measurements have been performed to determine the molecular coverage and the adsorption structure,

as detailed earlier.^{22,23} Angle-resolved photoelectron spectroscopy (ARPES) has been performed with monochromatized He I α radiation (21.2 eV), and the work function of the samples has been determined from the width of the photoelectron spectra. The coverage of 1 ML has been determined as the most densely packed structure (i.e., the (6 $\bar{1}$,1 4) adsorption structure²²).

We have used density functional theory (DFT) in atomistic calculations to study the geometric and electronic properties of pentacene on the Cu(110) substrate. Since the molecule is planar in shape and is expected to bind to the substrate with its π electrons, the interaction is relatively weak and van der Waals interactions might play an important role in the molecule–substrate interaction. Therefore, we have employed, besides the traditional generalized gradient approximation (GGA) in the form of Perdew–Burke–Ernzerhof (PBE),²⁴ also the van der Waals density functional (vdW-DF) of Langreth, Lundqvist, and co-workers.²⁵ We have modeled the supercell of the substrate laterally with a periodicity of (8 \times 2), corresponding to a coverage of 0.78 ML, and four layers along the surface normal together with about 22 Å of vacuum between the two sides of the slab. A (2 \times 6 \times 1) equi-distance grid of k -points has been used in the surface calculations.

For the study of the potential energy surface upon diffusion, we have used the Vienna ab initio simulation package (VASP)²⁶ with the PBE-GGA. The interaction between the valence electrons and ionic cores is described by the projector augmented wave (PAW) method.^{27,28} A plane-wave energy cutoff of 400 eV has been used for all calculations, yielding a lattice constant of 3.655 Å for bulk Cu, close to other calculations (3.635 Å) and experiments (3.595 Å).²⁹ One pentacene molecule (C₂₂H₁₄) has been adsorbed along the [110] direction of the substrate at an initial height of 3.5 Å above the surface at various lateral positions. A few different, randomly chosen starting positions have been tried, and they lead practically to the same final result in terms of geometry and energy. Since the optimization of the atomic positions at several different configurations along the potential energy surface was very computationally demanding, the optimizations were stopped when forces reached 0.05 eV/Å. The change in the total energy was always less than 1 meV toward the end of an optimization. We have obtained the potential energy surface corresponding to pentacene diffusion on the Cu(110) substrate by keeping one carbon atom fixed along the high-symmetry direction [110] and relaxing all the other coordinates of the adsorbate and first three substrate layers. The fixed C atom was chosen to be the closest one to the surface and has been denoted as C10. By systematically varying the position of the C10, we map the potential energy surface of diffusion along the close-packed rows.

For the DFT analysis of the energetics, geometry, and electronic structure, we have employed the Quantum ESPRESSO package.³⁰ The vdW-DF have been used as the exchange-correlation functional. The lattice constant is 3.737 Å, comparing well with the result, 3.708 Å, from an earlier calculation with the same functional.²⁹ Ultrasoft pseudopotentials introduced by Vanderbilt³¹ have been used for the relaxation of the ionic structure and norm-conserving pseudopotentials for the analysis. We have started from the minimum-energy structure obtained during the calculation of the potential energy surface of diffusion and relaxed it until the forces on the atoms were smaller than 0.002 eV/Å.

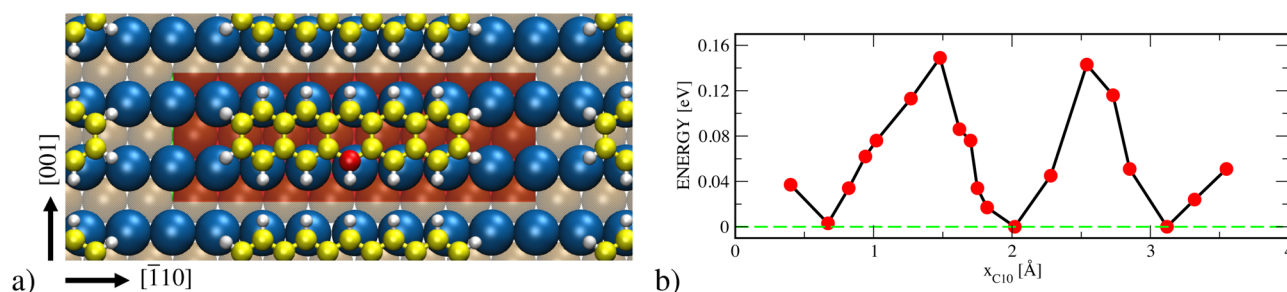


Figure 1. (a) Adsorption geometry of pentacene on Cu(110) optimized with the GGA-PBE functional. The unit cell is highlighted with the red-shaded rectangle and the topmost copper, carbon, and hydrogen atoms with blue, yellow, and white spheres, respectively. The carbon atom C10 closest to the surface is drawn with a red sphere. (b) Total energy profile from the GGA-PBE calculations as a function of the lateral position of the carbon atom C10 along the close-packed Cu rows. The red dots indicate the C10 atom lateral position. The potential energy surface is not completely symmetric along the x coordinate or the $[110]$ direction due to asymmetric values for x and possibly small hysteresis.

We have analyzed the electronic structure by calculating electron density differences: The electron densities of the isolated molecule and of the substrate have been subtracted from the electron density of the adsorption system

$$\Delta n(\mathbf{r}) = n_{\text{pc/Cu}}(\mathbf{r}) - n_{\text{pc}}(\mathbf{r}) - n_{\text{Cu}}(\mathbf{r}) \quad (1)$$

with the atomic coordinates as in the adsorbed structure and with the projection of the Kohn–Sham single-particle orbitals ψ_{ik} , where i is the band index and k the k point, onto the molecular orbitals of pentacene ϕ_{jk}

$$O_{jk}(E) = \sum_{ik} w_k |\langle \phi_{jk} | \psi_{ik} \rangle|^2 \delta(E - E_{ik}) \quad (2)$$

where E_{ik} is the Kohn–Sham eigenvalue corresponding to the state ψ_{ik} and w_k the weight of the k point. For an example of the analysis using this *orbital overlap*, please see ref 32. We note that it is particularly advantageous to use the orbital overlaps in the case of pentacene rather than the usual projected density of states (PDOS) because in the latter approach the wave functions of the full system are projected on the atomic orbitals of single atoms: In pentacene, however, all the frontier orbitals are of π type, yielding a similar p_z contribution for all these orbitals at a carbon atom. Therefore, the disentanglement of the different orbitals in the PDOS would be very difficult, whereas it is straightforward using the orbital overlaps.

To analyze the change in the surface dipole and its consequence in the work function, we introduce the one-dimensional electron density difference averaged along the surface planes

$$\Delta n_{1D}(z) = \int_y \int_x \Delta n(\mathbf{r}) dx dy / \left(\int_y \int_x dx dy \right) \quad (3)$$

RESULTS AND DISCUSSION

In Figure 1b, we show the energy versus the position of C10, the carbon atom closest to a substrate atom, along along $[110]$ obtained from GGA-PBE calculations. As a result of the detailed scrutiny paid to the energy landscape, we find that the pentacene/Cu(110) system exhibits two equilibrium adsorption sites that are symmetry-equivalent. Figure 1a shows a top view of one of these two adsorption sites that are separated by half of the nearest-neighbor distance of copper. The activation energy barrier for diffusion along the close-packed $[110]$ direction is 150 meV, as seen in Figure 1b. We did not attempt to determine the energy barrier for diffusion between neighboring channels, as the diffusion barrier is expected to

be much higher in this direction.³³ In both of the favored configurations, the adsorption energy of pentacene is 1.54 eV, with the molecule lying down bent in a “cradle” shape¹⁷ with the central carbon atoms sitting at 2.2 Å above the Cu surface while the carbon atoms at the extremities of the molecule sit 0.46 Å higher,²² as seen also in Figure 2a. On the substrate side, the adsorption of pentacene on Cu(110) changes the interlayer separation between the first and second layers only slightly. Since not all the surface copper atoms are sitting at the same height, this varies from -10% (1.16 Å) away from the adsorbant to -7% (1.20 Å) below it with respect to the bulk interlayer separation. The buckling within the first and second Cu(110) layers amounts to 0.11 and 0.15 Å, respectively. Hence, remarkably, the adsorption of pentacene on Cu(110) results in structural modifications on both sides of the interface which go beyond the expected level for a weakly adsorbed molecule with predominantly van der Waals interactions. We use the occurrence of such structural modifications as a first criterion for excluding “weak physisorption” interaction in this system.

The overall picture of adsorption geometry does not change when the vdW-DF is used. The adsorption energy at the most stable site increases to 1.79 eV, using a free molecule in a large unit cell as the reference. The separation between the C10 atom and the Cu atom beneath it is 2.29 Å, and the difference in height between them 2.25 Å. The carbon atoms at the end of the molecule are by 0.80 and 0.86 Å higher than the C10, in a curved geometry like with the GGA-PBE functional. The first layer of Cu is corrugated by 0.14 Å, and the average distance between the first and second layers is increased from 1.15 Å at the clean surface to 1.18 Å when the pentacene molecule is adsorbed.

In the following, we only present the results from the calculations with the vdW-DF functional, as the GGA-PBE results are very similar and support the same conclusions. Further results with GGA-PBE are given in the Supporting Information for more in-depth comparison.

The strong bending of the molecule²² (cf. Figure 2a) indicates that the carbon atoms interact with the substrate in a nonequivalent footing: those closer to the substrate will bind stronger than those further away. Consequently, the “binding energy per atom”, as established for the discussion of adsorption strengths and adsorption mechanisms, does not provide a complete criterion in the case of pentacene on Cu(110).

In search of a second criterion for the chemisorption-like interaction of pentacene on Cu(110), we investigate the

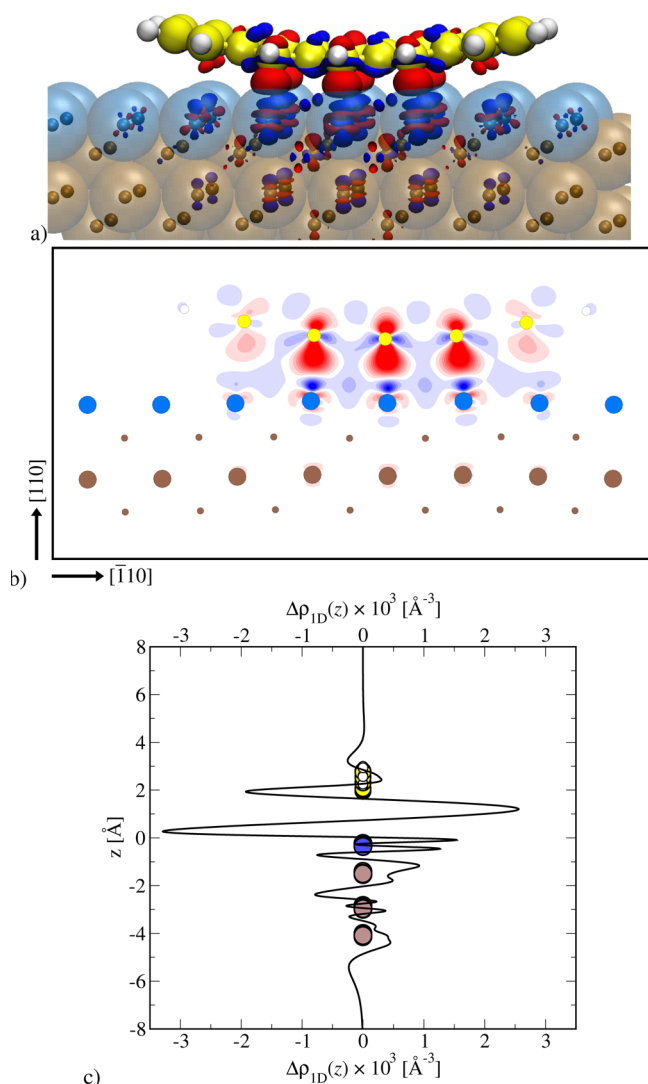


Figure 2. Difference in electron density upon adsorption of pentacene on Cu(110) obtained from the calculations with the vdW-DF. White spheres indicate hydrogen, yellow carbon, blue topmost layer substrate, and brown deeper layer substrate atoms. (a) Three-dimensional representation; the blue regions correspond to decreased and the red regions to increased electron density. (b) A cut of the electron density difference in the plane containing the surface normal and passing through the carbon atom C10. The atoms near this plane have been marked with large circles and the substrate layers further away from the plane with smaller circles. (c) The density difference averaged over the planes parallel to the surface.

changes in the electronic properties upon adsorption. Molecular adsorption always involves to a lesser or higher degree rearrangements of the electronic charge density on both sides of the interface, as it can be often recognized in changes of the surface dipole or work function.

In Figure 2, we thus show the rearrangement in the charge density in our calculations upon the adsorption. When there is charge depletion (i.e., electron accumulation) as compared to the isolated molecule or substrate, the charge difference appears in red, while the blue color represents charge accumulation (electron depletion). The accumulation of electron density below the pentacene molecule and the depletion of surface electrons at the Cu(110) substrate provide evidence for a substantial molecule/substrate interaction. The substrate

electrons are shifted from what looks like the $d_{3z^2-r^2}$ type orbitals, recognized in Figure 2a and b as blue regions above and below the Cu atoms in addition to a circle in the plane parallel to the surface, to $d_{xz,yz}$ type orbitals that display two circular red regions diagonally above and below the Cu atoms. The largest change at the pentacene molecule is the increased electron density at the π -electron system, mostly below the molecule toward the surface atoms, also appearing clearly in Figure 2c. Beyond these rearrangements, there is a weaker depletion of electrons in the molecular plane of the pentacene and above every second pair of carbon atoms along the molecule, displaying as red lobes above those atoms. These carbon atoms are the ones that are not in close contact with the substrate atoms.

Our DFT calculation implies a charge transfer of 0.8 electrons into the pentacene when using the Bader analysis^{34,35} to assign the electron density to the atoms, which corresponds to a 40% filling of the LUMO. A naïve view would suggest that the negative charge in the Bader volume of the molecule should increase the surface dipole and thus the work function upon pentacene adsorption on Cu(110) because charge density is brought further away from the surface. The charge redistribution upon pentacene interaction with the substrate is actually accompanied by a decrease of the work function by 0.29 eV as determined from our calculations. This value is in qualitative agreement with our experimentally measured values: for clean Cu(110), the work function was found to be 4.5 eV, while for a pentacene-covered surface a value of 3.6 eV was found at coverages of 0.7 and 1 ML.²³ The discrepancy between the calculated and experimental values is not explained by the lower coverage of pentacene considered in the simulation compared to the one in experiment but is more likely due to the shortcomings of the exchange-correlation functionals used. The change of the local work function alone is, however, no criterion to distinguish between chemisorption and physisorption, since also polarization due to van der Waals interaction induces work function changes.

The charge density difference in Figure 2 could have its origin in a redistribution of the electron densities. At the organic/metal interface, it is usually the modification of the densities of states near the Fermi level which determines the extent of electronic changes brought by the molecular adsorption. Therefore, we analyze the chemistry of adsorption using the orbital overlaps O in eq 2: These are shown in Figure 3 for the frontier orbitals of pentacene.

From Figure 3, it is obvious that the HOMO-1, HOMO, and LUMO have undergone splittings upon adsorption: HOMO-1 presents two main peaks at about 2.65 and 1.45 eV below the Fermi energy, HOMO a weak one at 2.20 and a stronger one at 0.85 eV below the Fermi energy, and LUMO at 2 eV below and one at the Fermi energy. The other orbitals of the pentacene molecule do not experience large splittings. Since there are no orbital degeneracies in the free pentacene molecule,³⁶ the splittings appear due to hybridization of the molecular orbitals with the electronic wave functions of the substrate, and thus originate from the chemical interaction (as opposed to just a rigid shift of energies due to the nearly homogeneous electrostatic field away from the substrate) at the interface. A more detailed analysis of the hybridization from the viewpoint of the substrate is given in the Supporting Information.

We also note that the position of the main peak of $O_{LUMO}(E)$ just below the Fermi energy explains the charge transfer from the substrate to the molecule, as this 2-fold degenerate state is

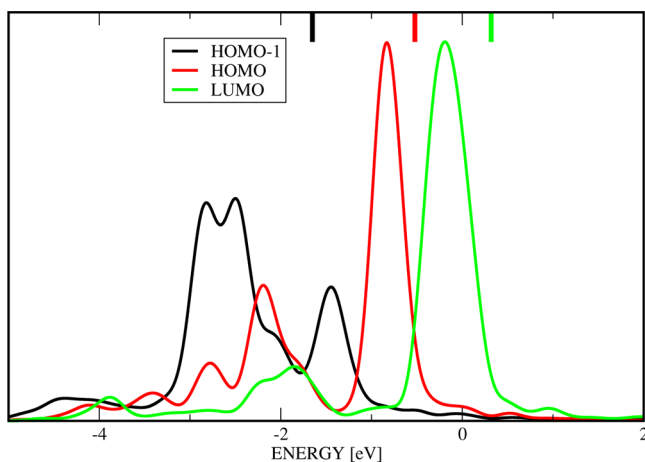


Figure 3. Projection of the Kohn–Sham states on the molecular orbitals, or the orbital overlap $O(E)$. The short vertical lines below the top axis denote the eigenvalues of the corresponding orbitals when the substrate is removed.

partially occupied. When no van der Waals interactions are taken into account (i.e., by using the GGA functional), the same qualitative behavior is found, though the corresponding hybrid peaks show up at somewhat larger binding energies (cf. the Supporting Information).

Our result for the orbital overlap does not agree with the DFT analysis in ref 16 on Cu(100), since there the LUMO state is well below the Fermi energy and would thus mean a charge transfer of two electrons to the molecule, which would be very large. Further, the electron state shown in ref 16 does not have the full symmetry of the adsorption system. In another article from the same authors,³⁷ the LUMO lies close to the Fermi energy at the $\bar{\Gamma}$ point but clearly at a lower energy at the \bar{X} point. In the DFT calculations on Cu(111) in ref 38, the density difference looks qualitatively similar to ours in Figure 2a, with the difference that on Cu(111) the molecule is flat whereas in our case on Cu(110) it is bent. The projection on molecular orbitals on Cu(111) yields also a similar result as on Cu(110), and the lowering of the work function on both surfaces agree qualitatively. The comparison of the properties of pentacene on Cu(111) and Cu(110) is complicated by the weaker adsorption on the former, leading to DFT results that strongly depend on the exchange–correlation functional and even the different treatments of the van der Waals interactions.³⁸ On Cu(110), where the bonding is stronger, the different DFT treatments are subsequently more consistent, as we have shown above.

The charge redistribution discussed above and the emergence of new hybridized states near the Fermi level are indications of a strong interaction which we use to qualify the interaction of pentacene with Cu(110) as chemisorption-like.

We have performed experimental studies to support the theoretical findings described above. Figure 4 shows angular resolved photoemission spectra of pentacene on Cu(110), which have been taken to derive the electronic states and their dispersion for different pentacene coverages and for the clean substrate. The inset on the top left shows the area of the surface Brillouin zone (SBZ) which has been mapped as well as the orientation of the azimuthal angle (cf. dotted arrow in the inset of Figure 4). The white dashed lines in the photoemission spectra indicate the SBZ boundaries. Two coverages corresponding to the (7×2) structure (0.7 ML), that is actually a

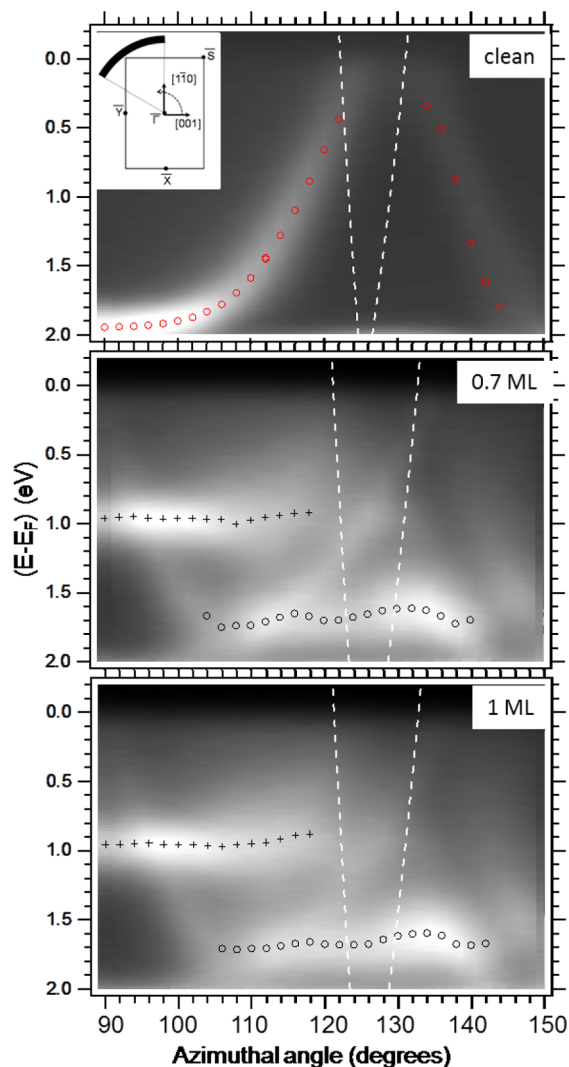


Figure 4. Angular resolved He I α valence band photoemission at a polar angle of 51.2° as a function of the azimuthal angle for the clean Cu(110) and two different pentacene coverages. The circles and crosses indicate the positions of the peak maxima derived from a Gaussian fit of the EDCs. The top left inset shows the angle scan with respect to the surface Brillouin zone and the arrow the orientation of the azimuthal angle scale. The molecule-derived bands at 0.96 (0.94) and 1.68 (1.67) eV at 0.7 (1.0) ML pentacene on Cu(110) are identified to be hybridized states derived from the HOMO and HOMO-1 molecular orbitals.

mobile structure with molecules diffusing along the $[\bar{1}10]$ direction, and the $(6 \bar{1}, 1 4)$ structure (1 ML) as shown in ref 22 have been analyzed. The cut across the SBZ has been chosen off normal at a polar angle of 51.2° starting from $\bar{\Gamma}$ – \bar{X} , as the hybridization states are not visible along the $\bar{\Gamma}$ – \bar{Y} direction and normal to the surface due to symmetry selection rules.³⁹ Compared to the fast dispersing sp band of the clean Cu(110) (cf. Figure 4), the pentacene induced bands—at 0.94 and 1.67 eV (for 1 ML) and at 0.96 and 1.68 eV (for 0.7 ML) binding energy—show only a weak dispersion of 90 meV (1 ML)/80 meV (0.7 ML) for the state closer to the Fermi energy and 120 meV (1 ML)/140 meV (0.7 ML) for the lower lying state. This indicates electron localization, and that electron hopping between molecules must be weak, since the pentacene induced bands show only a small dispersion in the investigated section.

The fact that no sizable difference, neither in dispersion nor in binding energy of the two states between adsorption of 0.7 and 1 ML of pentacene, could be measured shows that those states are related to the molecular orbitals and the bonding to the substrate, i.e., to interface states, and do not derive from intermolecular interactions, which are expected to be distinct for different coverages. The observation that the work function only decreases up to a coverage of approximately 0.7 ML and remains constant with further increasing coverage indicates that the average dipole induced in the molecules by their interaction with the surface decreases in transition from the low density molecular layer to higher densities which is related and in line with the observation of a complex phase evolution of pentacene on Cu(110) and corresponding electronic effects at the surface.^{22,23} At 0.7 ML, all molecules adsorb in the same position with respect to the substrate, whereas at the 1 ML coverage four different adsorption positions shifted by 1/4 of the unit cell in the $[\bar{1}10]$ direction are observed.^{22,23} Our experimental findings are in line with studies reported by Yamane et al.³⁹ who investigated a mixture of $p(6,5 \times 2)$ and $c(13 \times 2)$ phases, although they show a slightly stronger dispersion of approximately 250 meV for the state closer to the Fermi level which lies between 0.7 and 0.95 eV according to their measurements. These differences may be related to the different areas of the SBZ maps and to the fact that their samples have been annealed after pentacene adsorption while our samples have not been annealed during or after pentacene deposition.

The strong HOMO and the HOMO-1 hybrid states at 0.85 and 1.45 eV in Figure 3 can be assigned to the two states found in the experiment at 0.95 and 1.68 eV binding energy. The small discrepancies in the theoretical peak positions and the splitting of 0.61 eV, as compared to 0.73 eV from the experiment, are probably due to errors in the eigenvalues of the exchange-correlation functionals that we have employed, and due to possible photoemission final state relaxations,⁴⁰ which is also known for pentacene in the gas phase.⁴¹

The LUMO hybrid state at 0.19 eV below the Fermi energy in Figure 3 is more difficult to observe with photoemission because it lies close to the Fermi level. Before we describe our method for the determination of peaks near the Fermi energy, we mention that the second derivative, as applied in ref 39, is not suited for the measurement of peak positions near a discontinuity such as the Fermi edge. Here the data have been normalized with an empirical Fermi function that accounts for temperature and instrumental resolution.⁴² In order to make the LUMO visible in the data of Figure 4, we chose the average spectrum in the region between the azimuthal angles of 90 and 110° where no copper band crosses the Fermi level. From these spectra, the constant background well above the Fermi level has been subtracted. Subsequently, the spectra were normalized with the empirical Fermi function as obtained from the clean Cu data. Figure 5 shows the resulting normalized energy distribution curves for clean Cu, and at the two pentacene coverages. We find a peak at 20 ± 30 and 70 ± 25 meV above the Fermi energy for 0.7 and 1.0 ML pentacene, respectively. This is in good agreement with the expectation of a LUMO occupancy of 40%. The slightly lower energy of the 0.7 ML as compared to the 1 ML system is in line with the lower energy of the HOMO at 0.7 ML. We propose that the weak weight of the LUMO peak is related to matrix element effects,⁴³ and that it might be enhanced if the correct photon energy and the best k -space section are chosen.

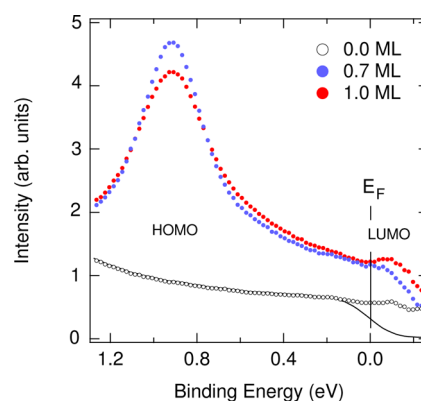


Figure 5. Photoemission spectra taken in a section without direct copper transitions. The data are normalized with an effective Fermi function. The peaks 20 (70) meV above the Fermi energy are assigned to the center of the LUMO for 0.7 (1.0) monolayer pentacene on Cu(110). The black solid line and open circles represent the data of the clean (0.0 ML) system prior to and after the normalization, respectively.

CONCLUSION

In summary, we have investigated the adsorption of pentacene on Cu(110), in direct comparison of experiment and theory, as a model system for the adsorption of a relatively large organic molecule on a metal surface. The interaction of the molecule with the substrate leads to considerable modifications, i.e., to reduced integrity of the atomic and electronic structure which imposes a substantial bending of the molecule and a buckling of the substrate top layers. The molecular bending substantially reduces the number of carbon and copper atoms, forming the bond across the interface. Because of this nonequivalency in the bonding between adsorbate atoms, the widely used “energy per atom” quantity is of limited use for the discussion of the strength of the bond, i.e., also of noncovalent bonds between large organic molecules and a metal substrate.

Thus, two characteristic effects, the hybridization at the vicinity of the Fermi level and charge redistribution between substrate and molecule, and the distortion of molecular conformation as well as of the Cu surface atoms provide unambiguous evidence for a significantly stronger adsorption than typical for van der Waals physisorption. We conclude that these effects can be taken as indicators for the enhanced, chemisorption-like interaction of large organic molecules with a metallic substrate. This interaction and its structural and electronic side effects at the organic–metal interface is a crucial determinant of organic electronic devices, thereby motivating further in depth studies.

ASSOCIATED CONTENT

Supporting Information

Molecular frontier orbitals and symmetries of pentacene molecule. Analysis of electron density and orbital overlap with the GGA functional and a thicker slab with vdW-DF. Analysis of the electronic states of the substrate participating in the hybridization. This material is available free of charge via the Internet at <http://pubs.acs.org>.

AUTHOR INFORMATION

Corresponding Author

*E-mail: Abdelkader.Kara@ucf.edu.

Present Address

[†]Zernike Institute for Advanced Materials, University of Groningen, Nijenborgh 4, NL-9747 AG Groningen, Netherlands.

Notes

The authors declare no competing financial interest.

ACKNOWLEDGMENTS

A.K. acknowledges support from the Department of Energy (grant DE-FG02-11ER16243) and UCF in-house funding and thanks the University of Zurich and the Paul Scherrer Institute for hospitality.

REFERENCES

- (1) Horowitz, G. *J. Mater. Res.* **2004**, *19*, 1946–1962.
- (2) Witte, G.; Wöll, C. *J. Mater. Res.* **2004**, *19*, 1889–1916.
- (3) Editorial, *Nat. Mater.* **2009**, *8*, 691.
- (4) Szulcowski, G.; Sanvito, S.; Coey, M. *Nat. Mater.* **2009**, *8*, 693–695.
- (5) Dediu, V.; Huego, L.; Bergenti, I.; Taliani, C. *Nat. Mater.* **2009**, *8*, 707–716.
- (6) Stingelin, N. *Nat. Mater.* **2009**, *8*, 858–860.
- (7) Alves, H.; Molinari, A.; Xie, H.; Morpurgo, A. *Nat. Mater.* **2008**, *7*, 574–580.
- (8) Duhm, S.; Heimel, G.; Salzman, I.; Glowatzki, H.; Johnson, R.; Vollmer, A.; Rabe, J.; Koch, N. *Nat. Mater.* **2008**, *7*, 326–332 and references therein.
- (9) Braun, S.; Salaneck, W.; Fahlmann, M. *Adv. Mater.* **2009**, *21*, 1450–1472.
- (10) Vanoni, C.; Tsujino, T. *J. S. Appl. Phys. Lett.* **2009**, *94*, 253306.
- (11) Vanoni, C.; Tsujino, S.; Jung, T. *Appl. Phys. Lett.* **2007**, *90*, 193119.
- (12) Ali, M. E.; Sanyal, B.; Oppeneer, P. M. *J. Phys. Chem. C* **2009**, *113*, 14381–14383.
- (13) Venables, J. *Introduction to Surface and Thin Film Processes*; Cambridge University Press: 2009.
- (14) Kara, A.; DePristo, A. *J. Chem. Phys.* **1988**, *88*, 2033–2035.
- (15) Koch, N. *J. Phys.: Condens. Matter* **2008**, *20*, 184008.
- (16) Ferretti, A.; Baldacchini, C.; Calzolari, A.; Felice, R. D.; Ruini, A.; Molinari, E.; Betti, M. *Phys. Rev. Lett.* **2007**, *99*, 046802.
- (17) Jung, T. A.; Schlittler, R. R.; Gimzewski, J. *Nature* **1997**, *386*, 696–698.
- (18) Woodruff, D. P. *J. Phys.: Condens. Matter* **1994**, *6*, 6067–6094.
- (19) Gimzewski, J. K.; Jung, T. A.; Cuberes, M. T.; Schlittler, R. R. *Surf. Sci.* **1997**, *386*, 101–114.
- (20) Schunack, M.; Linderoth, T. R.; Rosei, F.; Lægsgaard, E.; Stensgaard, I.; Besenbacher, F. *Phys. Rev. Lett.* **2002**, *88*, 156102.
- (21) Greber, T.; Raetz, O.; Kreutz, T.; Schwaller, P.; Deichmann, W.; Wetli, E.; Osterwalder, J. *Rev. Sci. Instrum.* **1997**, *68*, 4549–4554.
- (22) Müller, K.; Kara, A.; Kim, T. K.; Bertschinger, R.; Scheybal, A.; Osterwalder, J.; Jung, T. A. *Phys. Rev. B* **2009**, *79*, 245421.
- (23) Scheybal, A.; Müller, K.; Bertschinger, R.; Wahl, M.; Bendounan, A.; Aebi, P.; Jung, T. A. *Phys. Rev. B* **2009**, *79*, 115406.
- (24) Perdew, J. P.; Burke, K.; Ernzerhof, M. *Phys. Rev. Lett.* **1996**, *77*, 3865–3868.
- (25) Langreth, D. C.; Lundqvist, B. I.; Chakarova-Käck, S. D.; Cooper, V. R.; Dion, M.; Hyldgaard, P.; Kelkkanen, A.; Kleis, J.; Kong, L.; Li, S. J. *Phys.: Condens. Matter* **2009**, *21*, 084203.
- (26) Kresse, G.; Furthmüller, J. *Phys. Rev. B* **1996**, *54*, 11169–11186.
- (27) Blöchl, P. *Phys. Rev. B* **1994**, *50*, 17953–17979.
- (28) Kresse, G.; Joubert, D. *Phys. Rev. B* **1999**, *59*, 1758–1775.
- (29) Klimes, J.; Bowler, D. R.; Michaelides, A. *Phys. Rev. B* **2011**, *83*, 195131.
- (30) Giannozzi, P.; Baroni, S.; Bonini, N.; Calandra, M.; Car, R.; Cavazzoni, C.; Ceresoli, D.; Chiarotti, G. L.; Cococcioni, M.; Dabo, I. *J. Phys.: Condens. Matter* **2009**, *21*, 395502.
- (31) Vanderbilt, D. *Phys. Rev. B* **1990**, *41*, 7892–7895.
- (32) Lorente, N.; Hedoui, M. F. G.; Palmer, R. E.; Persson, M. *Phys. Rev. B* **2003**, *68*, 155401.
- (33) Yildirim, H.; Kara, A.; Durukanoglu, S.; Rahman, T. *Surf. Sci.* **2006**, *600*, 484–492.
- (34) Bader, R. *Atoms in Molecules: a Quantum Theory*; Oxford University Press: 1990.
- (35) Tang, W.; Sanville, E.; Henkelman, G. *J. Phys.: Condens. Matter* **2009**, *21*, 084204.
- (36) The symmetry group of the flat pentacene molecule is D_{2h} , which does not have any two- or higher-dimensional irreducible representations. Thus, no degeneracies (beyond accidental ones) are possible in the gas phase, and all the orbitals carry maximally only spin-degeneracy. Therefore, even the bending of the molecular geometry does not lead to the appearance of any new peaks in the density of states, and all the splittings in orbital projections are due to hybridization with the electrons of the substrate. The bending from the planar, gas-phase structure to the adsorption structure reduces the energy spacing of the unoccupied orbitals relative to the occupied ones. The shift of frontier orbitals LUMO and LUMO+1 with respect to HOMO and HOMO-1 is about 0.35 eV (cf. Figure 5 in the Supporting Information).
- (37) Baldacchini, C.; Mariani, C.; Betti, M. G.; Vobornik, I.; Fujii, J.; Anese, E.; Rossi, G.; Ferretti, A.; Calzolari, A.; Di Felice, R.; et al. *Phys. Rev. B* **2007**, *76*, 245430.
- (38) Toyoda, K.; Hamada, I.; Lee, K.; Yanagisawa, S.; Morikawa, Y. *J. Chem. Phys.* **2010**, *132*, 134703.
- (39) Yamane, H.; Yoshimura, D.; Kawabe, E.; Sumii, R.; Kanai, K.; Ouchi, Y.; Ueno, N.; Seki, K. *Phys. Rev. B* **2007**, *76*, 165436.
- (40) Morscher, M.; Seitsonen, A. P.; Ito, S.; Takagi, H.; Dragoe, N.; Greber, T. *Phys. Rev. A* **2010**, *82*, 051201.
- (41) Endres, R. G.; Fong, C. Y.; Yang, L. H.; Witte, G.; Wöll, C. *Comput. Mater. Sci.* **2004**, *29*, 362–370.
- (42) Cepek, C.; Sancrotti, M.; Greber, T.; Osterwalder, J. Electronic structure of K-doped C_{60} monolayers on Ag(001). *Surf. Sci.* **2000**, *454–456*, 467–471.
- (43) Puschnig, P.; Reinisch, E.-M.; Ules, T.; Koller, G.; Soubatch, S.; Ostler, M.; Romaner, L.; Tautz, F.; Ambrosch-Draxl, C.; Ramsey, M. Orbital tomography: Deconvoluting photoemission spectra of organic molecules. *Phys. Rev. B* **2011**, *84*, 235427.